OPEN ACCESS

International
Journal
Of Modern Engineering Research (IJMER)

Generalized Torus Helix Method Design of Hydrodynamic Torque Converter Stator

Liu Shipng[1,2], Zheng Shujuan[1], Wei Yeshu[1]
[1](Department of Mechanical Engineering, North China University of Water Resources and Electric Power, China)
[2](Department of Mechanical Engineering, Shangqiu Institute of Technology, China)

ABSTRACT: *The stator design method was investigated. A new design method, generalized torus helix design method, was proposed. The generalized torus helix equation of stator was established. The equation reflecting the interrelationship among polar angle, blade angle and offset angle was derived. Four different functions were used for blade design. How to assess a design scheme of flow field was studied. The maximal curvature, exit curvature and maximal offset angle served as the original parameters of scheme assessment. Normalized parameters are used to calculate assessment indexes. The scheme selecting mechanism of flow field design reasonability was put forward. Hyperbolic sine function was determined as offset angle function. Vector calculus and thickness function were used to compute blade surface coordinates. A parameterized design program code was developed. All equations were verified. Investigation results state that generalized torus helix design method is feasible and substantially accurate results can be obtained. The program can not only draw camber surface and blade surfaces automatically, but also output a solid of revolution and flow passage surface coordinates so as to model conveniently. Therefore, the investigation provides a parameterized and approximately optimum method for stator design and is of application value.*

Keywords: *Hydrodynamic Torque Converter, Generalized Torus Helix Method, Scheme Selecting Mechanism, Hyperbolic Sine, Vector Calculus, Approximately Optimum design.*

I. INTRODUCTION

Hydrodynamic torque converters are widely used in power transmission chains of various vehicles. The three basic elements of a torque converter are a pump, a turbine and a stator, respectively. The main advantage of a torque converter is able to vary rotational speed and torque automatically. Therefore, the traction performance of the vehicle is improved greatly. In addition, the vibration damping and absorbing performance of liquid can enhance comfortable performance of the vehicle and prolong the service life of transmission components. However, an evident disadvantage of a hydrodynamic torque converter is that its efficiency is not high enough. Since several million torque converters are built every year, even a small improvement in efficiency would result in significant fuel savings [1].

A hydrodynamic torque converter is a complex geometry. In addition, the liquid flow inside a torque converter is highly three-dimensional(3D), viscous and turbulent. Furthermore, the pump and turbine rotate at different angular velocity. For these reasons, the flow field of a torque converter is extremely complex. On the other hand, since a number of variables are involved in the design of a torque converter, it is difficult to achieve an optimal design[2]. In order to understand the flow behavior inside a torque converter, many scholars have made their best efforts. The performance of the torque convertor was numerical investigated, including the integrated design strategy [2] and the distributed parameter strategy for the internal flow filed, for instance, the boundary element method [3]. Many experimental studies were also carried out to improve the performance of torque convertors, for example, laser velocimetry method [4], laser sheet lighting method [5], particle image velocimetry (PIV) method [6] and the method using a miniature conventional five-hole probe [7], etc. These researchers mainly focused on the flow field inside the torque convertor. The influence of the key factor, such as the stator/reactor blade [4, 5, 6, 8, 9], and the speed ratio [7], was investigated.

Actually, the 3D streamline of flow field is an underlying factor that has great influence on the efficiency. Even if the fluid particle velocity magnitude does not change, the change of its velocity direction (streamline curvature) will cause power loss. This loss is proportional to the abruptness of velocity change [10]. The accumulation effect of the unit inertia force to its path is constant and independent of the intermediate path, which

was indirectly inferred that the energy loss is relative with maximal streamline curvature [11]. In order to reduce the energy loss, the perfect line type of a 3D streamline should be a straight line segment or a circular arc. Ref. [12] utilized arcs and straight line segments as streamlines. As a result, the energy losses resulting from streamline curvature decreased greatly. However, because stator blade angle variation from entrance to exit is very large and the stator flow passage is substantially short, it was unfeasible for the arcs and straight line segments to serve as 3D streamlines via mathematical verification [13]. Besides straight line segments and circular arcs, helixes possess constant or approximate constant curvatures. Naturally, helixes should be chosen as 3D streamlines.

In this paper, a new stator design method, generalized torus helix design method, was proposed. The helix equation was derived. Four different functions were used for stator design. A feasible scheme selecting mechanism was established. Vector calculus and thickness function were used to compute blade surface coordinates. This investigation provided a parameterized and approximately optimized method of stator design.

II. MERIDIONAL PATH LINE EQUATION

For the complex geometry of a torque converter, the coordinate system suitable to flow field description is the generalized torus coordinate system [14]. The space position of a fluid particle can be determined with a polar angle θ, a polar radius ρ and an offset angle ϕ. The meridional flow path equation is given by:

$$\rho = h\frac{\sqrt{(1+\delta\sin\theta)^2+2\xi\sigma\sin\theta}-1}{\sin\theta} \tag{1}$$

If $\xi=-1$, the meridional flow path denotes core contour line; if $\xi=0$, the meridional flow path denotes design path; if $\xi=1$, the meridional flow path denotes shell contour line.

The revolution radius is:

$$r = h\sqrt{(1+\delta\sin\theta)^2+2\xi\sigma\sin\theta} \tag{2}$$

III. GENERALIZED TORUS HELIX EQUATION

The schematic of generalized torus helix is shown as in Fig.1.

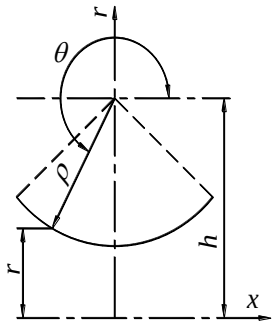

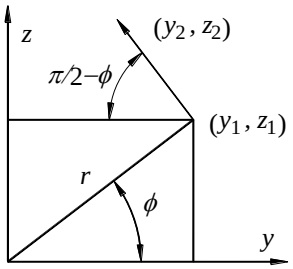

Fig.1. Schematic of generalized torus helix **Fig.2**. Unit circumferential velocity vector

From Fig.1, the helix equation can be written as following:

$$\begin{cases} x = \rho\cos\theta \\ y = r\cos\phi \\ z = r\sin\phi \end{cases} \tag{3}$$

where offset angle $\phi = \mathrm{f}(\theta)$ is an undetermined function.

If blade span parameter ξ takes on a constant, equation (3) actually is a 3D streamline equation. If blade span parameter ξ varies continuously, equation (3) actually is a 3D stream surface equation. In the design process of stator blade, equation (3) can be considered as a camber surface equation as well.

IV. DETERMINATION OF OFFSET ANGLE FUNCTION

A unit circumferential velocity vector is constructed as shown in Fig.2. From Fig.2, it can be seen that the unit circumferential velocity vector take the form:

$$\mathbf{n} = (0, y_2 - y_1, z_2 - z_1) = (0, -\sin\phi, \cos\phi)$$

If the tangential vector of a 3D streamline is expressed as $(\Delta x, \Delta y, \Delta z)$, the formula of blade angle is given by:

$$\cos\beta = \lim_{\Delta\theta\to 0} \frac{(\Delta x, \Delta y, \Delta z)\cdot(0, -\sin\phi, \cos\phi)}{|(\Delta x, \Delta y, \Delta z)|\cdot|(0, -\sin\phi, \cos\phi)|}$$

Rewrite the above expression, yielding:

$$\cos\beta = \frac{-(\mathrm{d}y/\mathrm{d}\theta)\sin\phi + (\mathrm{d}z/\mathrm{d}\theta)\cos\phi}{\sqrt{(\mathrm{d}x/\mathrm{d}\theta)^2 + (\mathrm{d}y/\mathrm{d}\theta)^2 + \mathrm{d}z/\mathrm{d}\theta)^2}} \tag{4}$$

The derivatives of three coordinates and revolution radius with respect to polar angle are:

$$\begin{cases} x' = r'/\tan\theta - (r-h)/\sin^2\theta \\ y' = r'\cos\phi - r\phi'\sin\phi \\ z' = r'\sin\phi + r\phi'\cos\phi \\ r' = h^2(\delta + \xi\sigma + \delta^2\sin\theta)\cos\theta / r \end{cases} \tag{5}$$

Substitute the above derivatives into equation (4), yielding:

$$\cos\beta = r\phi'(x'^2 + r'^2 + r^2\phi'^2)^{-1/2} \tag{6}$$

or

$$\beta = \arctan\{[(x'/r)^2 + (r'/r)^2]/\phi'\} \tag{7}$$

From equation (7), it can be seen that the blade angle is relative with the first order derivative of the offset angle, rather than the value of the offset angle. In other words, as long as the entrance blade angle and exit blade angle are specified, more than one function can serve as an offset angle function, which provides multifold selection for stator blade design.

For the stator blade, because both curvature and tension are substantially high, it is more reasonable to apply inverse potential flow criterion[15,16] for blade design. In this manner, the maximal offset angle of the stator blade can be reduced. The expression of inverse potential flow criterion is:

$$v_u / r = v_{ud} / r_d \tag{8}$$

Thus, the blade angle relationship on two different flow paths is:

$$\cot\beta = g\cot\beta_d \tag{9}$$

where coefficient $g = \sqrt{1 + \xi[2\sigma\sin\theta/(1+\delta\sin\theta)^2]}$.

At the entrance and exit, the corresponding factors are:

$$g_1 = \sqrt{1 + \xi[2\sigma\sin\theta_1/(1+\delta\sin\theta_1)^2]}$$
$$g_2 = \sqrt{1 + \xi[2\sigma\sin\theta_2/(1+\delta\sin\theta_2)^2]}$$

In order to ensure the blade angles at the entrance and exit, the follows must be satisfied:

$$f'(\theta_1) = \sqrt{(x_1'/r_1)^2 + (r_1'^2/r_1)^2}\sqrt{1 + 2\xi\sigma\sin\theta_1/(1+\delta\sin\theta_1)^2}\cot\beta_1$$
$$f'(\theta_2) = \sqrt{(x_2'/r_2)^2 + (r_2'^2/r_2)^2}\sqrt{1 + 2\xi\sigma\sin\theta_2/(1+\delta\sin\theta_2)^2}\cot\beta_2$$

Obviously, $f'(\theta_1) \neq f'(\theta_2)$, which means that $\phi = f(\theta)$ must be nonlinear. The following functions can be selected.

(1) Parabola

Assume that $\phi = \mathrm{f}(\theta)$ is a parabola, the first and second order derivatives of offset angle with respect to polar angle take the form:

$$\begin{cases} \phi' = f'(\theta) = E + F\theta \\ \phi'' = F \end{cases} \tag{10}$$

where $F = [f'(\theta_2) - f'(\theta_1)]/(\theta_2 - \theta_1)$, $E = [\theta_2 f'(\theta_1) - \theta_1 f'(\theta_2)]/(\theta_2 - \theta_1)$.

Integrating equation (10) and applying boundary condition $\phi_1 = f(\theta_1) = 0$, we can obtain:

$$\phi = E(\theta - \theta_1) + F(\theta^2 - \theta_1^2)/2 \tag{12}$$

With the first order derivative of the offset angle, by using equation (7), the blade angle can be obtained. The curves of the offset angle and blade angle versus the polar angle can be plotted as shown in Fig.3.

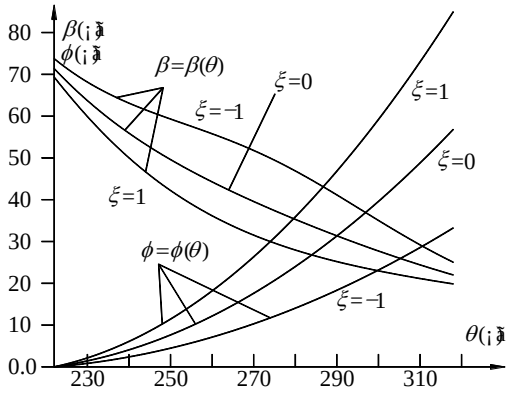

Fig.3. Curve of parabola type offset angle function

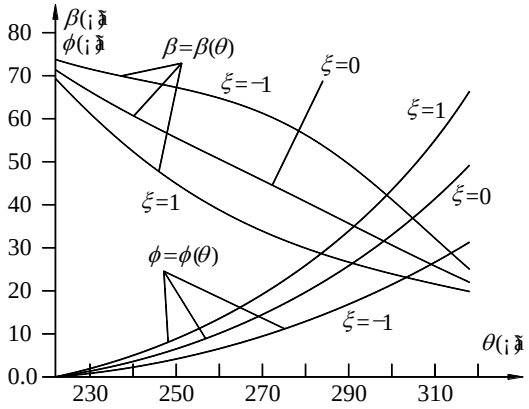

Fig.4. Curves of arc type offset angle function

(2) Circular arc

Assume that $\phi = f(\theta)$ is a circular arc and satisfies the following equations:

$$\phi = b - \sqrt{R^2 - (\theta - a)^2} \tag{13}$$

$$\phi' = (\theta - a)[R^2 - (\theta - a)^2]^{-1/2} \tag{14}$$

$$\phi'' = R^2[R^2 - (\theta - a)^2]^{-3/2} \tag{15}$$

Applying boundary conditions, we obtain:

$$\begin{cases} (\theta_1 - a)[R^2 - (\theta_1 - a)^2]^{-1/2} = f'(\theta_1) \\ (\theta_2 - a)[R^2 - (\theta_2 - a)^2]^{-1/2} = f'(\theta_2) \\ b - [R^2 - (\theta_1 - a)^2]^{1/2} = 0 \end{cases} \tag{16}$$

From the first two expressions of equation (16), it is given by:

$$(p_2 - p_1)a^2 - 2(p_2\theta_2 - p_1\theta_1)a + (p_2\theta_2^2 - p_1\theta_1^2) = 0$$

where $p_1 = 1 + 1/[f'(\theta_1)]^2$, $p_2 = 1 + 1/[f'(\theta_2)]^2$.

Solving the quadric equation, we have:

$$a = p + \sqrt{p^2 - q} \tag{17}$$

where $p = (p_2\theta_2 - p_1\theta_1)/(p_2 - p_1)$, $q = (p_2\theta_2^2 - p_1\theta_1^2)/(p_2 - p_1)$.

Once again, from equation (16), it is given by:

$$\begin{cases} b = (\theta_1 - a)/f'(\theta_1) \\ R^2 = b^2 + (\theta_1 - a)^2 \end{cases} \tag{18}$$

The curves of the offset angle and blade angle versus the polar angle are plotted as shown in Fig.4.

(3) Exponent

Consider the equation of an exponent function given below:

$$\phi = A(e^{k(\theta - \theta_1)} - 1) \tag{19}$$

By differentiating the above expression, the follows can be obtained:

$$\begin{cases} \phi' = Ake^{k(\theta - \theta_1)} \\ \phi'' = Ak^2e^{k(\theta - \theta_1)} \end{cases} \tag{20}$$

Applying boundary conditions, we have:

$$\begin{cases} Ak = f'(\theta_1) \\ Ake^{k(\theta_2-\theta_1)} = f'(\theta_2) \end{cases}$$

Solve the above equations, yielding:

$$\begin{cases} k = (\theta_2 - \theta_1)^{-1} \ln[f'(\theta_2)/f'(\theta_1)] \\ A = k^{-1} f'(\theta_1) \end{cases} \tag{21}$$

The curves of the offset angle and blade angle versus the polar angle can be plotted as shown in Fig.5.

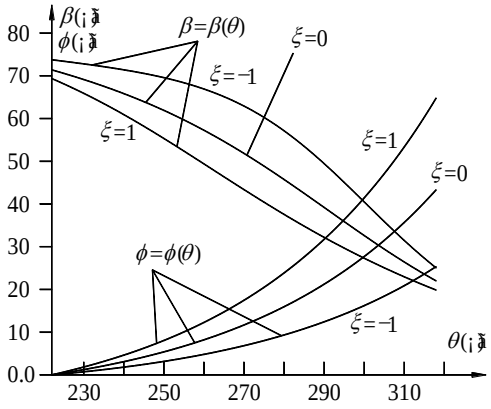

Fig.5. Curves of exponent type offset angle function

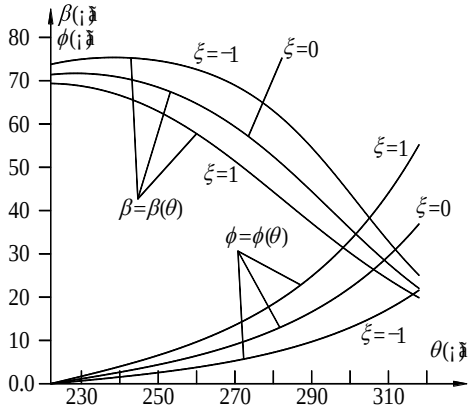

Fig.6. Curves of hyperbolic sine type offset angle function

(4) Hyperbolic sine

Assume that $\phi = f(\theta)$ is a hyperbolic sine and is expressed as following:

$$\phi = A\sinh[k(\theta - \theta_1)] \tag{22}$$

Differentiate the above expression, yielding:

$$\begin{cases} \phi' = Ak\cosh[k(\theta - \theta_1)] \\ \phi'' = Ak^2\sinh[k(\theta - \theta_1)] \end{cases} \tag{23}$$

Substituting the required derivative values at the entrance and exit, we have:

$$\begin{cases} Ak = f'(\theta_1) \\ Ak\cosh[k(\theta_2 - \theta_1)] = f'(\theta_2) \end{cases}$$

Solve the above equations, there resulting:

$$\begin{cases} k = (\theta_2 - \theta_1)\ln\left\{f'(\theta_2)/f'(\theta_1) + \sqrt{[f'(\theta_2)/f'(\theta_1)]^2 - 1}\right\} \\ A = k^{-1} f'(\theta_1) \end{cases} \tag{24}$$

The curves of the offset angle and blade angle versus the polar angle are plotted as shown in Fig.6.

V. COMPUTATION OF 3D STREAMLINE CURVATURE

The 3D streamline curvature is an underlying factor causing energy losses. The objective pursued in the design of flow field is to make the curvature reach its minimum. Therefore, it is important to quantitatively compute the curvature of a 3D streamline.

The curvature of a 3D streamline is defined as:

$$K = \frac{|\mathbf{V}' \times \mathbf{V}''|}{|\mathbf{V}'|^3} \tag{25}$$

where $\mathbf{V}' = (\mathrm{d}x/\mathrm{d}\theta, \mathrm{d}y/\mathrm{d}\theta, \mathrm{d}z/\mathrm{d}\theta)$, $\mathbf{V}'' = (\mathrm{d}^2x/\mathrm{d}\theta^2, \mathrm{d}^2y/\mathrm{d}\theta^2, \mathrm{d}z^2/\mathrm{d}\theta^2)$.

The second order derivatives of coordinates and revolution radius with respect to polar angle are:

$$\begin{cases} x'' = r''/\tan\theta + 2(x - r')/\sin^2\theta \\ y'' = (r'' - r\phi'^2)\cos\phi - (2r'\phi' + r\phi'')\sin\phi \\ z'' = (r'' - r\phi'^2)\sin\phi + (2r'\phi' + r\phi'')\cos\phi \\ r'' = (h^2\delta^2\cos 2\theta - h^2\varepsilon\sin\theta - r'^2)/r \end{cases} \tag{26}$$

Let $p = r', q = r\phi', u = r'' - r\phi'^2, v = 2r'\phi' + r\phi''$, **we have:**

$$\begin{cases} y' = p\cos\phi - q\sin\phi \\ z' = p\sin\phi + q\cos\phi \\ y'' = u\cos\phi - v\sin\phi \\ z'' = u\sin\phi + v\cos\phi \end{cases} \tag{27}$$

Therefore, the curvature calculation formula of a 3D streamline is given by:

$$K = [(pv - qu)^2 + (px'' - ux')^2 + (qx'' - vx')^2]^{1/2}[(x')^2 + p^2 + q^2]^{-3/2} \tag{28}$$

Corresponding to the parabola scheme, arc scheme , exponent scheme and hyperbolic sine scheme, curvature values of 3D streamlines can be obtained with the help of the program, and be plotted into curves as shown in Fig.7, 8, 9 and 10, respectively.

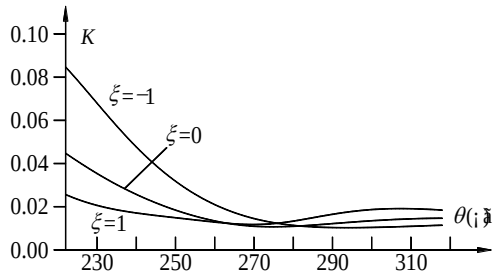

Fig.7. Curvature curves corresponding to parabola scheme

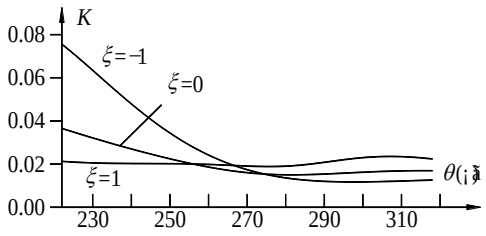

Fig.8. Curvature curves corresponding to arc scheme

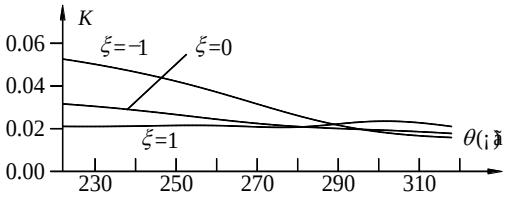

Fig.9. Curvature curves corresponding to exponent scheme

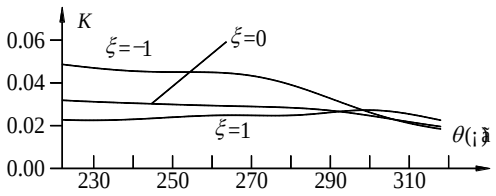

Fig.10. Curvature curves corresponding to hyperbolic sine

VI. ASSESSMENT OF DESIGN SCHEME

How to assess the four schemes is vitally important. Several factors should be taken into account. The first factor is the maximal curvature of 3D streamlines. The 3D streamline curvature is relative with energy loss. The higher the streamline curvature is, the larger energy loss. In order to enhance the efficiency of a hydrodynamic torque converter, the best effort must be made so as to reduce the maximal curvature of 3D streamlines. The second factor is the maximal offset angle at the exit. It is the maximal offset angle that decides whether it is difficult for the stator to be fabricated or not. The third is if it is reasonable for blade angle to vary. More importantly, the blade variation in the vicinity of exit has influence on flow deflection that causes deflection loss. Therefore, the exit curvature of 3D streamlines should serve as an assessment parameter as well.

With the help of the program code, three assessment parameters, maximal curvature, exit curvature and maximal offset angle, can be computed, as tabulated in Table 1

Table 1. Maximal curvatures, exit curvatures and maximal offset angles of 3D streamlines

Offset angle function scheme No.	Maximal curvature	Exit curvature	Maximal offset angle (°)
1	0.0846588	0.0184538	84.9789
2	0.0755536	0.0223780	66.3262
3	0.0526234	0.0210314	64.7931
4	0.0486598	0.0225488	55.2345

From Table1, it can be noted that, from scheme one to scheme four, both maximal curvature and maximal offset angle are decrease gradually; whereas the exit curvature is increases gradually. A good scheme is that all the three parameters reach their minimum. Obviously, it is uneasy to take our choice merely according to Table 1.

On the other hand, because the order of magnitude of three assessment parameters is different, it is inconvenient to compare these schemes. Therefore, the three parameters of all the schemes need be normalized.

The above table can be considered as a matrix $\mathbf{A}$. The average value of each column is:

$$a_j = \frac{1}{4}\sum_{i=1}^{4} A_{i,j} \tag{29}$$

If each datum is divided by the average value of the column data, we can obtain a new matrix **B**:

$$B_{i,j} = A_{i,j} / a_j \tag{30}$$

In this manner, the normalized values of assessment parameter can be obtain, as tabulated in Table 2

Table 2: Normalized parameters and assessment indexes

scheme No.	Normalized Maximal curvature	Normalized exit curvature	Normalized Maximal offset angle	product index	sum index
1	1.29500	0.87447	1.25276	1.41866	3.42223
2	1.15572	1.06042	0.97778	1.19832	3.19392
3	0.80496	0.99661	0.95518	0.76628	2.75675
4	0.74433	1.06851	0.81427	0.64761	2.62711

With normalized assessment parameters, the four schemes can be assessed quantitatively. The first assessment index is product index. The product index is given by:

$$p_i = \prod_{j=1}^{3} B_{i,j} \tag{31}$$

The second assessment index is sum index. The sum index is given by:

$$s_i = \sum_{j=1}^{3} B_{i,j} \tag{32}$$

Program computation results indicate that both the product index and sum index point to scheme 4, or hyperbolic sine function scheme.

Once again，from Table 1 it is can be found that hyperbolic sine applied as offset angle function can significantly reduce maximal curvature and maximal offset angle. In adverse aspects, the variation of blade angle is unreasonable and the exit curvatures of 3D streamlines are slightly high.

On the other hand, from Fig.10, it can be noted that the curvature curves in the vicinity of entrance are close to horizontal lines, which indicates that the hyperbolic sine scheme is close to an optimum design scheme.

VII. DETERMINATION OF BLADE THICKNESS VECTOR

The camber surface expressed by equation (4) can be considered as a two variable function with respect to polar θ and blade span parameter ξ.

The tangential vector of the camber surface along stream wise is:

$$\mathbf{V}_1 = (\partial x/\partial\theta, \partial y/\partial\theta, \partial z/\partial\theta) \tag{33}$$

$$\partial x/\partial\theta = (\partial r/\partial\theta)/\tan\theta - (r-h)/\sin^2\theta$$
$$\partial y/\partial\theta = (\partial r/\partial\theta)\cos\phi - r(\mathrm{d}\phi/\mathrm{d}\theta)\sin\phi$$
$$\partial z/\partial\theta = (\partial r/\partial\theta)\sin\phi + r(\mathrm{d}\phi/\mathrm{d}\theta)\cos\phi$$

Take the partial derivative of revolution radius with respect to polar angle, yielding:

$$\partial r/\partial\theta = (h^2/r)(\varepsilon + \delta^2\sin\theta)\cos\theta$$

where $\varepsilon = \delta + \xi\sigma$.

Substitute $\partial r/\partial\theta = (h^2/r)(\varepsilon+\delta^2\sin\theta)\cos\theta$ **into the foregoing expression, yielding:**

$$\partial x/\partial\theta = h^2(\varepsilon+\delta^2\sin\theta)\cos^2\theta/(r\sin\theta) - (r-h)/\sin^2\theta$$
$$\partial y/\partial\theta = h^2\cos\phi - r\sin\phi\phi'$$
$$\partial z/\partial\theta = h^2[(\varepsilon+\delta^2\sin\theta)\cos\theta/r]\sin\phi + r\cos\phi\phi'$$

The tangential vector of the camber surface along the blade span wise is given by:

$$\mathbf{V}_2 = (\partial x/\partial\xi, \partial y/\partial\xi, \partial z/\partial\xi) \tag{34}$$

where $\partial x/\partial\xi = (\partial r/\partial\xi)/\tan\theta$, $\partial y/\partial\xi = (\partial r/\partial\xi)\cos\phi$, $\partial z/\partial\xi = (\partial r/\partial\xi)\sin\phi$.

Substituting $\partial r/\partial\xi = (h^2\sigma/r)\sin\theta$ **into above expressions，there results:**

$$\partial x/\partial\xi = (\partial r/\partial\xi)/\tan\theta = (h^2\sigma/r)\cos\theta$$
$$\partial y/\partial\xi = (\partial r/\partial\xi)\cos\phi = (h^2\sigma/r)\sin\theta\cos\phi$$
$$\partial z/\partial\xi = (\partial r/\partial\xi)\sin\phi = (h^2\sigma/r)\sin\theta\sin\phi$$

The blade thickness vector $\mathbf{V}$ is equal to the cross product of vector $\mathbf{V}_1$ and $\mathbf{V}_2$

$$\mathbf{V} = \mathbf{V}_1\times\mathbf{V}_2 = v_x i + v_y j + v_z k \tag{35}$$

where $v_x = (\partial y/\partial\theta)(\partial z/\partial\xi) - (\partial z/\partial\theta)(\partial y/\partial\xi) = -h^2\sigma\sin\theta\phi'$

$v_y = (\partial z/\partial\theta)(\partial x/\partial\xi) - (\partial x/\partial\theta)(\partial z/\partial\xi) = h^2\sigma[(\rho/r)\sin\phi + \cos\theta\cos\phi\phi']$

$v_z = (\partial x/\partial\theta)(\partial y/\partial\xi) - (\partial y/\partial\theta)(\partial x/\partial\xi) = -h^2\sigma[(\rho/r)\cos\phi - \cos\theta\sin\phi\phi']$

$|\mathbf{V}| = h^2\sigma[(\rho/r)^2 + \phi'^2]^{1/2}$

VIII. DETERMINATION OF BLADE THICKNESS FUNCTION

Assume that a blade of the stator is enveloped with different diameter balls. Each ball diameter is the function of polar angle, as shown in Fig.11.

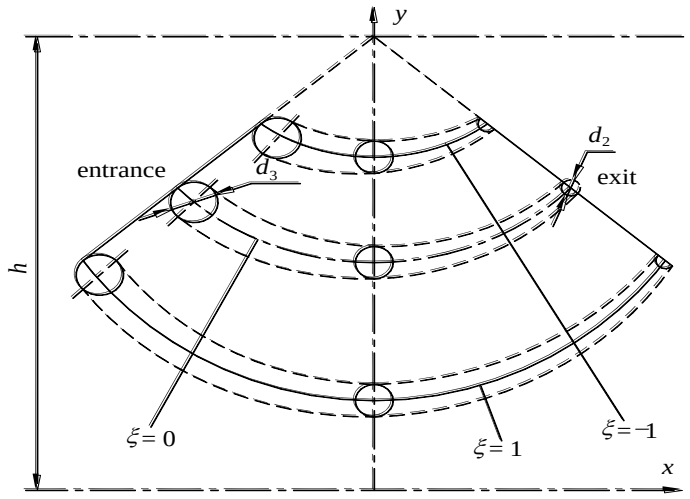

Fig.11. Schematic of stator blade thickness

From entrance to exit, the ball diameter decreases gradually from maximal diameter d_3 to minimal diameter d_2. If polar angle $\theta = \theta_1$, the diameter $d = 0$; If polar angle $\theta = \theta_3$, the diameter $d = d_3$; if $\theta = \theta_2$, the diameter $d = d_2$. In order to establish the function relationship of the ball diameter d with respect to polar angle θ, in advance, it is necessary to obtain the polar angle θ_3 corresponding to maximal ball diameter d_3.

It is difficult to directly find polar angle θ_3. A feasible method is to obtain two integer angle θ_L and θ_R, where $\theta_R - \theta_L = 1°$ and $\theta_L \le \theta_3 \le \theta_R$. At this stage, an approximate solution can be obtained by using dichotomy.

In the case of $(\theta_3 \le \theta \le \theta_2)$, assume that the ball diameter varies linearly. It is given by:

$$d = d_3 + (d_2 - d_3)(\theta - \theta_3)/(\theta_2 - \theta_3)$$

In the case of $(\theta_1 \le \theta \le \theta_3)$, a equivalent ball diameter is used to calculate blade thickness, as shown in Fig.12.

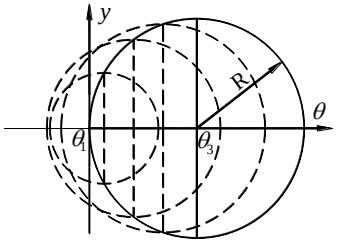

Fig.12. Blade thickness in the vicinity of entrance

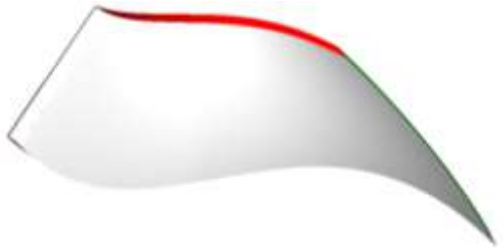

Fig.13. Three-dimensional blade of the stator

From Fig.12, it can be find that the radius of maximal circle is:

$$R = \theta_3 - \theta_1$$

The equation of the maximal circle is:

$$(\theta - \theta_3)^2 + y^2 = R^2$$

For any $\theta < \theta_3$, y -coordinate is given by:

$$y = \sqrt{R^2 - (\theta - \theta_3)^2}$$

The equivalent ball diameter of blade thickness is:

$$d = (y/R)d_3$$

Combining the above two expressions, we have:

$$d = \begin{cases} d_3\sqrt{1-[(\theta-\theta_3)/(\theta_3-\theta_1)]^2} & (\theta < \theta_3) \\ d_3 + (d_2 - d_3)(\theta - \theta_3)/(\theta_2 - \theta_3) & (\theta \ge \theta_3) \end{cases} \quad (36)$$

With the help of the program and graphic interface, a 3D blade of a stator can be drawn automatically, as shown in Fig.13.

IX. CONCLUSION

The stator design method was investigated. Some main results are as follows:

1) A new design method, generalized torus helix design method, was proposed and the generalized torus helix equation of 3D streamline was established.
2) The equation reflecting the function relationship among polar angle, blade angle and offset angle was derived.
3) The assessment selecting mechanism of flow field design reasonability was put forward.
4) Hyperbolic sine function serves as offset angle function, which is close to an optimum design scheme.
5) Vector calculus and thickness function were used to compute blade surface coordinates. Substantially accurate results can be obtained.
6) The parameterized program can not only draw the camber surface and blade surfaces automatically, but also output a solid of revolution and the flow passage surface coordinates so as to model conveniently.

In summary, the investigation provides a parameterized and approximately optimum method for stator design, and is of application value.

ACKNOWLEDGMENT

This project is supported by Henan Provincial Tackle Key Program of China (Grant No. 0424260038) and Henan Key Scientific Research Projects in Colleges and Universities of China (Grant No.16A460020).

NOMENCLATURE

h =distance from the arc center of design path to the shaft center
θ =polar angle
θ_1 =polar angle at the entrance

θ_2 =polar angle at the exit

θ_3 =polar angle corresponding to the maximal diameter ball

d =ball diameter

ρ =polar radius

σ =constant

δ =constant, $\delta = R / h$

R =geometric radius of design path

ξ =blade span parameter

ϕ = offset angle

v_{ud} =circumferential component velocity of absolute velocity on the design path

v_u =circumferential component velocity of absolute velocity on any other meridional flow path

r_d =revolution radius on the design path

r =revolution radius on any other meridional flow path

β_d =blade angle on the design path.

β =blade angle on any other meridional flow path.

g =coefficient.

z_n =blade number of stator

ψ = one half of center angle of flow passage

REFERENCES

[1]. Liu Y. F., Lakshminarayana B. and Burningham J.. Flow Field in the Turbine Rotor Passage in an Automotive Torque Converter Based on the High Frequency Response Rotationg Five-hole Probe Measurement, Part I: Flow Field at the Design Condition(Speed Ratio 0.6). International Journal of Rotating Machinery, 7(4), 2001, 253-269.

[2]. Yang S., Shin S., Bae I. and Lee T., Takeyung Lee. A Computer-integrated Design Strategy for Torque Converters Using Virtual Modeling and Computational Flow Analysis, SAE Paper No. 1999-01-1046, 1999.

[3]. Yamada M., Imai K., Iwaki T. Numerical Analysis of the Torque Converter Stator Blade by the Boundary Element Method, SAE Paper No. 921692, 1992.

[4]. Ainley S. B., and Flack R. D. Laser Velocimeter Measurements in the Stator of an Automotive Torque Converter, International Journal of Rotating Machinery, 6(6),2000, 417-431.

[5]. Watanabe H., Kurahashi T. and Kojima M. Flow Visualization and Measurement of Torque Converter Stator Blades Using a Laser Sheet Lighting Method and a Laser Doppler Velocimeter, SAE Paper No. 970680, 1997.

[6]. Kunisaki Y., Kobayashi T., Saga T., Taniguchi N., Segawa S., Kajitani K., Fukunaga T. and Tasaka T. PIV Measurement on the Flow Field around a Stator Cascade of Automotive Torque Converter, SAE Paper No. 2001-01-0868, 2001.

[7]. Dong Y., Lakshminarayana B. Experimental Investigation of the Flow Field in an Automotive Torque Converter Stator, Journal of Fluids Engineering, 121(4), 788-797, 1999.

[8]. Shin S., Kim K. J., Kim D. J., Joo I. S., Hong J. H. and Jang Y. K. The Effect of Reactor Blade Geometry on the Performance of an Automotive Torque Converter, SAE Paper No. 2002-01-0885, 2002.

[9]. Kim G., Jang J. Effects of Stator Shapes on Hydraulic Performances of an Automotive Torque Converter with a Squashed Torus, SAE Paper No. 2002-01-0886, 2002.

[10]. Daugherty R. L., Franzini J. B. Fluid Mechanics with Engineering Application (McGraw-Hill Inc., New York,1977).

[11]. Liu S. P., Quan L. Minimum Curvature Design of Three-Element Centripetal-turbine Hydrodynamic Torque Converters, Journal of China Ordnance, 5(2), 20-24, 2009.

[12]. Liu S. P., Zheng S. J. Three-dimensional Streamline Design of the Flow Passage of Hydrodynamic Torque Converter, International Journal of Modern Engineering Research (IJMER), 4(8), 11-18, 2014.

[13]. Liu S. P., Zhao X. S. Plane Streamline Method Design of Hydrodynamic Torque Converter. Third International Conference on Theoretical and Mathematical Foundations of Computer Science, Bali, Indonesia, 2012, 914-920.

[14]. Liu S. P., Quan L. Mathematical Model of Hydrodynamic Torque Converter and Analytic Description of Streamline, Chinese Journal of Mechanical Engineering, 22(1), 70-77, 2009.

[15]. Jandasek V. J. The Design of a Single-stage Three-element Torque Converter, SAE Paper No. 610576, 1961.

[16]. Ma W. X. Hydrodynamic transmission theory and design (Chemical Industry Press, Peking, China, 2004).